THE SCHWARZ ALTERNATING METHOD FOR MULTISCALE CONTACT MECHANICS

JONATHAN HOY*, IRINA TEZAUR†, AND ALEJANDRO MOTA‡

Abstract. Contact is an important research topic in the study of mechanical systems. State-of-the-art computational methods for simulating mechanical contact are prone to numerical difficulties, leading to poor performance (in terms of simulation time and accuracy) and a lack of robustness. Here, we describe and evaluate a novel approach for simulating contact based on the Schwarz alternating method. With this method, contact constraints are replaced with boundary conditions that are applied iteratively on the contact boundaries. Results from a canonical impact problem with an exact analytical solution suggest that the new Schwarz methodology has the potential to offer a significant improvement to established approaches.

1. Introduction. An important aspect of simulating mechanical systems, whether engineered or natural, is understanding a given system's behavior when subjected to contact under normal or abnormal environments (e.g., touching surfaces, sliding, tightened bolts, impact, etc.). Whereas the methods and tools for simulating the bulk behavior of mechanical systems are well-developed and mature, the same cannot be said for contact mechanics. This situation is due to the complexity of the contact phenomenon itself and associated numerical difficulties. Traditionally, for computational simulation, the contact problem is divided into two steps: a proximity search, and the enforcement of contact constraints (introduced to prevent interpenetration of objects coming into contact). The proximity search is primarily a computer science problem, and has received much attention due to its paramount importance in other fields such as video game development. In relative terms, less attention has been devoted to the enforcement step, a multiscale physics phenomenon due primarily to the microscopic and macroscopic features of contact surfaces. Existing computational methods available for enforcement suffer from poor performance, both in terms of simulation timeand solution accuracy, and can lead both to long wait times and to physically incorrect predictions. Although traditionally, most of the computational expense in contact simulations is associated with the proximity search, there is also room for improvement when it comes to the efficiency of enforcement algorithms.

This paper introduces and evaluates numerically a fundamentally new approach to simulating mechanical contact based on the domain decomposition-based Schwarz alternating method [18]. The new approach leverages our previous work in Schwarz multiscale coupling [15, 16] and addresses two well-known problems in computational simulation of contact: (1) the accuracy of the contact constraint enforcement, and (2) the multiple scales involved. Rather than introducing contact constraints into the variational form of the problem, as done in conventional contact techniques, e.g., the penalty method [11, 6], the Lagrange multiplier method [3, 1] and the augmented Lagrangian method [1, 20, 26], the Schwarz alternating method decomposes the problem domain into two or more subdomains and prevents interpenetration by applying transmission (boundary) conditions in an iterative and alternating fashion on the subdomain boundaries. As shown in our earlier work [15, 16], the Schwarz alternating method has a number of desirable qualities, including its ability to use different element topologies and time integrators in different subdomains. We demonstrate herein

*University of Southern California, hoyj@usc.edu
†Sandia National Laboratories, ikalash@sandia.gov
‡Sandia National Laboratories, amota@sandia.gov

that these advantageous properties carry over to the contact variant of the method.

Toward this effect, the remainder of this paper is organized as follows. Section 2 describes the variational formulation of the generic solid mechanics problem considered herein, and details its spatio-temporal discretization. Section 3 presents our new Schwarz alternating contact formulation, which relies on non-overlapping subdomains and alternating Dirichlet-Neumann boundary conditions. Numerical results on a one-dimensional (1D) impact problem with an exact analytical solution are given in Section 4. The use of the 1D problem allows the investigation of the Schwarz algorithm as a viable contact method, circumventing other issues that are common to most contact algorithms, such as projection of fields from one contact surface to another. In addition to the Schwarz alternating method, we evaluate the performance of three conventional contact algorithms: the implicit and explicit penalty methods [11, 6], and the explicit Lagrange multiplier method (also known as the forward increment Lagrange multiplier method) [3]. Although the augmented Lagrangian method [1, 20, 26] is a popular approach for simulating mechanical contact, we do not consider this method in the present work. Our results demonstrate that the Schwarz alternating method predicts various quantities of interest (e.g., the contact point displacement, the impact and release time, the system energies) and conserves total energy better than the conventional contact methods, but introduces some oscillations in the contact point velocity and contact point forces. Ideas for minimizing these oscillations and general avenues for future work are discussed in Section 5.

2. Solid mechanics problem formulation. Consider the Euler-Lagrange equations for a generic dynamic solid mechanics problem in its strong form:

$$\operatorname{Div} \boldsymbol{P} + \rho_0 \boldsymbol{B} = \rho_0 \ddot{\boldsymbol{\varphi}} \quad \text{in} \quad \Omega \times I. \tag{2.1}$$

In (2.1), $\Omega \in \mathbb{R}^d$ for $d \in \{1, 2, 3\}$ is an open bounded domain, $I := \{t \in [t_0, t_1]\}$ is a closed time interval with $t_0 < t_1$, and $\boldsymbol{x} = \boldsymbol{\varphi}(\boldsymbol{X}, t) : \Omega \times I \to \mathbb{R}^d$ is a mapping, with $\boldsymbol{X} \in \Omega$ and $t \in I$, $\boldsymbol{P}$ denotes the first Piola-Kirchhoff stress, and $\rho_0 \boldsymbol{B} : \Omega \to \mathbb{R}^3$ is the body force, with ρ_0 denoting the mass density in the reference configuration. The over-dot notation denotes differentiation in time, so that $\dot{\boldsymbol{\varphi}} := \frac{\partial \boldsymbol{\varphi}}{\partial t}$ and $\ddot{\boldsymbol{\varphi}} := \frac{\partial^2 \boldsymbol{\varphi}}{\partial t^2}$. Embedded within $\boldsymbol{P}$ is a constitutive model, which can range from a simple linear elastic model to a complex micro-structure model, e.g., that of crystal plasticity.

Suppose that we have the following initial and boundary conditions for the partial differential equations (PDEs) (2.1):

$$\begin{gathered} \boldsymbol{\varphi}(\boldsymbol{X}, t_0) = \boldsymbol{X}_0, \;\; \dot{\boldsymbol{\varphi}}(\boldsymbol{X}, t_0) = \boldsymbol{v}_0 \text{ in } \Omega, \\ \boldsymbol{\varphi}(\boldsymbol{X}, t) = \boldsymbol{\chi} \text{ on } \partial\Omega_{\boldsymbol{\varphi}} \times I, \;\; \boldsymbol{P}\boldsymbol{N} = \boldsymbol{T} \text{ on } \partial\Omega_{\boldsymbol{T}} \times I. \end{gathered} \tag{2.2}$$

In (2.2), it is assumed the outer boundary $\partial\Omega$ is decomposed into a Dirichlet and traction portion, $\partial\Omega_{\boldsymbol{\varphi}}$ and $\partial\Omega_{\boldsymbol{T}}$, respectively, with $\partial\Omega = \partial\Omega_{\boldsymbol{\varphi}} \cup \partial\Omega_{\boldsymbol{T}}$ and $\partial\Omega_{\boldsymbol{\varphi}} \cap \partial\Omega_{\boldsymbol{T}} = \emptyset$. The prescribed boundary positions or Dirichlet boundary conditions are $\boldsymbol{\chi} : \partial\Omega_{\boldsymbol{\varphi}} \times I \to \mathbb{R}^3$. The symbol $\boldsymbol{N}$ denotes the unit normal on $\partial\Omega_{\boldsymbol{T}}$.

It is straightforward to show that the weak variational form of (2.1) with initial and boundary conditions (2.2) is

$$\int_I \left[\int_\Omega (\operatorname{Div} \boldsymbol{P} + \rho_0 \boldsymbol{B} - \rho_0 \ddot{\boldsymbol{\varphi}}) \cdot \boldsymbol{\xi} \; \mathrm{d}V + \int_{\partial_{\boldsymbol{T}}\Omega} \boldsymbol{T} \cdot \boldsymbol{\xi} \; \mathrm{d}S \right] \mathrm{d}t = 0, \tag{2.3}$$

where $\boldsymbol{\xi}$ is a test function in $\mathcal{V} := \left\{ \boldsymbol{\xi} \in W_2^1(\Omega \times I) : \boldsymbol{\xi} = \boldsymbol{0} \text{ on } \partial_{\boldsymbol{\varphi}}\Omega \times I \cup \Omega \times t_0 \cup \Omega \times t_1 \right\}$.

Discretizing the variational form (2.3) in space using the classical Galerkin finite element method (FEM) [10] yields the following semi-discrete matrix problem:

$$\boldsymbol{M}\ddot{\boldsymbol{u}} + \boldsymbol{f}^{\text{int}} = \boldsymbol{f}^{\text{ext}}. \tag{2.4}$$

In (2.4), $\boldsymbol{M}$ denotes the mass matrix, $\boldsymbol{u} := \boldsymbol{\varphi}(\boldsymbol{X}, t) - \boldsymbol{X}$ is the displacement, $\ddot{\boldsymbol{u}}$ is the acceleration, $\boldsymbol{f}^{\text{ext}}$ is a vector of applied external forces, and $\boldsymbol{f}^{\text{int}}$ is the vector of internal forces due to mechanical and other effects inside the material. In the case of a problem with mechanical contact that is formulated with traditional contact methods, $\boldsymbol{f}^{\text{ext}}$ includes a contact contribution derived from a contact constraint, which must be enforced effectively.

A fully discrete problem is obtained by applying to (2.4) a time-integration scheme. A popular choice of time-integration scheme for solid mechanics problems such as those considered herein is the Newmark-beta method [17]. This scheme can be either first or second order accurate, depending on the values of its parameters β and γ. Additionally, it can be either implicit (and therefore unconditionally stable) or explicit, again depending on the values of β and γ.

3. The Schwarz alternating method. The purpose of the present work is to introduce and evaluate a *new* approach for simulating mechanical contact. This new approach is based on the Schwarz alternating method, an iterative domain decomposition-based approach that was first proposed in 1870 by Schwarz [18]. As mentioned earlier, in [15] and [16], the authors developed the Schwarz alternating method as a means for enabling continuum-to-continuum coupling in quasistatic and dynamic solid mechanics, respectively. In these works, the physical domain Ω is decomposed into two or more overlapping subdomains (Figure 3.1(a)), and the governing PDEs are solved within each subdomain in an iterative fashion, with information propagating through Dirichlet boundary conditions on the so-called Schwarz boundaries (Γ_1 and Γ_2 in Figure 3.1(a)). The method was shown to have a number of advantages over classical monolithic discretizations, enabling the seamless coupling in a plug-and-play manner of different mesh resolutions, different element types, and even different time integration schemes without introducing spurious errors or artifacts. Additionally, the method was shown to have a provable convergence guarantee [15, 16].

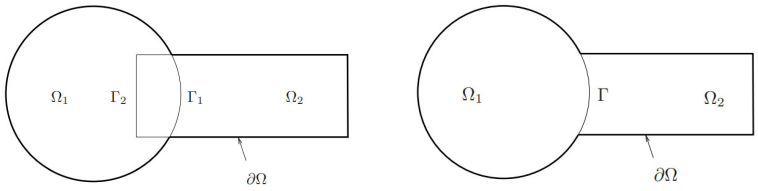

(a) Overlapping (b) Non-overlapping

FIG. 3.1. *Illustration showing overlapping and non-overlapping domain decomposition.*

3.1. Formulation. Motivated by the earlier work [15, 16] and the observation that a contact problem can be viewed as a coupled problem while two or more bodies are in contact, we propose herein to transform the Schwarz alternating method into a fundamentally new approach for simulating mechanical contact. A typical contact

configuration is shown in Figure 3.1(b). The reader can observe that the configuration of interest involves two non-overlapping domains, connected by the contact boundary, denoted by Γ in this figure. Extending the Schwarz alternating method to contact problems hence requires extending the method's formulation to the case of non-overlapping subdomains. As first demonstrated in the late 1980s by Lions [13] and Zanolli *et al.* [25], obtaining a provably-converging Schwarz method for the case of non-overlapping domains requires specialized transmission conditions. Specifically, whereas Dirichlet-Dirichlet transmission conditions ensure convergence in the case of overlapping domains, a convergent formulation in the non-overlapping domain case can be obtained by prescribing either Robin-Robin [13, 9, 8, 5, 14] or alternating Dirichlet-Neumann [25, 7, 4, 12] boundary conditions on Γ (Figure 3.1(b)). In the present formulation, we consider the latter approach, which translates to alternating displacement-traction boundary conditions for the mechanical problem (2.3).

Consider, without loss of generality, a problem involving two subdomains, denoted by Ω_1 and Ω_2, that have come into contact, as depicted in Figure 3.1(b). Once contact has been detected using a global search algorithm based on specified contact conditions (described in Section 3.2), we begin the Schwarz iteration process. Following the Schwarz alternating method for transient solid dynamics [16], the present Schwarz alternating formulation includes the notion of a so-called "controller time stepper", which defines a set of global time-steps, denoted by $\triangle T$, at which the subdomains are synchronized (for more details, see Section 2.2 of [16]). For the specific case of (2.3), two subdomains and a controller time interval I_N, the Schwarz iteration takes the form:

$$\begin{cases} \boldsymbol{M}_1\ddot{\boldsymbol{u}}_1^{n+1} + \boldsymbol{f}_1^{\text{int;n+1}} = \boldsymbol{f}_1^{\text{ext;n+1}} \\ \qquad\qquad\qquad \boldsymbol{\varphi}_1^{n+1} = \boldsymbol{\chi}, \text{ on } \partial_{\boldsymbol{\varphi}}\Omega_1\backslash\Gamma, \\ \qquad\qquad\qquad \boldsymbol{\varphi}_1^{n+1} = \boldsymbol{\varphi}_2^{n}, \text{ on } \Gamma, \end{cases} \quad \begin{cases} \boldsymbol{M}_2\ddot{\boldsymbol{u}}_2^{n+1} + \boldsymbol{f}_2^{\text{int;n+1}} = \boldsymbol{f}_2^{\text{ext;n+1}} \\ \qquad\qquad\qquad \boldsymbol{\varphi}_2^{n+1} = \boldsymbol{\chi}, \text{ on } \partial_{\boldsymbol{\varphi}}\Omega_2\backslash\Gamma, \\ \qquad\qquad\qquad \boldsymbol{T}_2^{n+1} = \boldsymbol{T}_1^{n+1}, \text{ on } \Gamma. \end{cases} \tag{3.1}$$

In (3.1), $n = 0, 1, 2, ...$ denotes the Schwarz iteration number and N denotes the controller time-step number. We select to develop the alternating Dirichlet-Neumann formulation of the non-overlapping Schwarz method over the Robin-Robin formulation, as Dirichlet and Neumann (traction) boundary conditions are readily available in most solid mechanics codes, e.g., Sandia's Sierra/Solid Mechanics (Sierra/SM) code [19]. Alternate formulations, such as the formulation with Robin-Robin transmission conditions and various formulations involving numerical relaxation (see [22] and the references therein), may be considered in future work. The iteration (3.1) continues until convergence is reached. It is emphasized that the formulation (3.1) does not require that a conformal discretization be used within the various subdomains; as for the multiscale Schwarz alternating method [15, 16], different discretizations, element types and even time-integration schemes can be used in different subdomains.

3.2. Contact criteria. An important part of any contact algorithm is defining a set of criteria to determine when contact has occurred. Herein, we consider the following set of contact criteria.

1. *Overlap condition*: triggered when two or more objects/domains have begun to overlap/penetrate each other.
2. *Push condition*: triggered when both of the following properties hold
   (a) *Compression*: the tractions at the interface are compressive.
   (b) *Sustainability*: there was contact in the previous time step.

Specifically, two or more bodies are determined to be in contact if either the overlap condition or the push condition hold.

The contact conditions enumerated above are roughly equivalent to the well-known Karush-Kuhn-Tucker (KKT) conditions [24, 26] appearing in traditional mechanical contact formulations. It is noted that, unlike traditional contact formulations (penalty [11, 6], Lagrange multiplier [3, 1], augmented Lagrangian methods [1, 20]), our Schwarz-based does not require the definition of contact constraints into the problem formulation.

4. Numerical results. The main contribution of this paper is the numerical evaluation of the Schwarz alternating method described in Section 3, as compared to several state-of-the-art contact approaches. Section 4.1 succinctly summarizes the methods evaluated herein. Following this discussion, we describe the benchmark problem on which these methods are studied (Section 4.2) and present numerical results for several variants of this problem (Sections 4.3–4.4).

4.1. Summary of contact methods evaluated. We restrict our attention herein to three classes of methods: (1) the penalty method [11, 6], (2) the Lagrange multiplier method [3, 1], and (3) the Schwarz alternating method (Section 3).

The penalty method [11, 6] is one of the simplest approaches for mechanical contact, and applies a contact force that is linearly proportional to the amount of interpenetration by means of a penalty parameter τ. The penalty method is popular since it is very easy to implement into existing mechanics frameworks, but has the downside of having its accuracy and stability properties affected greatly by the choice of the penalty parameter, for which there is no exact science. If the penalty parameter τ is too low, the amount of interpenetration allowed can be too high, yielding inaccurate results; in contrast, selecting a τ that is too high can affect adversely the overall numerical stability of the method and can lead to inaccuracies/oscillations in the contact forces. The penalty method can be run with either an implicit or an explicit time-stepping scheme, both of which are considered in the present study.

In the Lagrange multiplier method [3, 1], contact constraints are imposed weakly using Lagrange multipliers; hence, unlike in the penalty method, the contact conditions are satisfied more precisely and there is no empirical parameter to tune. Lagrange multiplier methods present their own challenges, however. Care must be taken to design the Lagrange multiplier finite element space such that the *inf-sup* condition [2] is upheld, and implementing this mixed method in existing high-performance computing (HPC) codes such as Sierra/SM [19] can be cumbersome. Additionally, the Lagrange multiplier formulation gives rise to an indefinite discrete saddle point problem, which can be difficult to solve numerically and may require specialized preconditioning schemes. In [3], Carpenter *et al.* developed a specific variant of the Lagrange multiplier method with explicit time-stepping known as the "forward increment Lagrange multiplier method", which has been shown to deliver superior results over implicit Lagrange multiplier formulations for impact problems. For this reason, we restrict attention herein to the explicit (forward increment) Lagrange multiplier method, and do not consider the implicit variant of this method.

An important aspect of conventional contact methods such as the penalty and Lagrange multiplier methods is that they require the specification of contact constraints imposed within their respective formulations. Herein, we impose the so-called zero gap constraint, which ensures that the gap between a given pair of objects is never negative and hence the objects do not interpenetrate. We note here that it is not uncommon to impose in place of or in conjunction with the zero gap constraint a second

constraint, namely that of a zero gap rate [23, 21]. The zero gap rate constraint was not considered in the numerical study performed herein, but would be an interesting future endeavor.

The Schwarz alternating method for simulating mechanical contact was described in Section 3. We evaluate herein three variants of the Schwarz alternating method: one in which an implicit Newmark-beta time-integration scheme is used in all subdomains, one in which an explicit Newmark-beta time-integration scheme is used in all subdomains, and one in which explicit and implicit Newmark-beta coupling is performed between the domains.

Table 4.1 summarizes the six methods evaluated in this paper.

TABLE 4.1
Summary of contact methods evaluated.

Method	Time-stepping scheme
Penalty	Implicit Newmark-beta
	Explicit Newmark-beta
Forward increment Lagrange multiplier [3]	Explicit Newmark-beta
Schwarz	Implicit-Implicit Newmark-beta
	Explicit-Implicit Newmark-beta
	Explicit-Explicit Newmark-beta

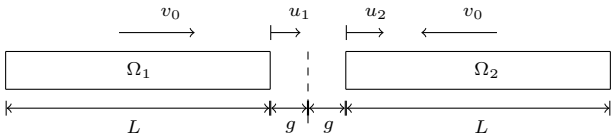

FIG. 4.1. *Illustration of 1D impact problem*

4.2. One-dimensional impact problem. The Schwarz alternating method described in Section 3 and the three existing state-of-the-art contact methods described in Section 4.1 are evaluated on a simple 1D problem involving the impact of two identical linear elastic prismatic rods having density ρ, elastic modulus E and cross-sectional area A moving with equal speed in opposite directions. This test case is a variant of the problem considered in Section 5 of [3], and has an exact analytical solution. The configuration is depicted in Figure 4.1. The rods are initially undeformed and the configuration is symmetric about the plane at which the two rod faces impact. Let v_0 denote the initial speed of each rod. Let L denote the length of each rod, and assume the rods are initially separated by a distance $2g$. Per the derivation in [3], it is straightforward to shows that the position and velocity of the right end of the left rod are given by

$$x(t) = \begin{cases} -g + v_0(t - t_0), & t < t_{\text{imp}}, \\ 0, & t_{\text{imp}} \le t \le t_{\text{rel}}, \\ -v_0(t - t_{\text{rel}}), & t > t_{\text{rel}}, \end{cases} \quad v(t) = \begin{cases} v_0, & t < t_{\text{imp}}, \\ 0, & t_{\text{imp}} \le t \le t_{\text{rel}}, \\ -v_0, & t > t_{\text{rel}}, \end{cases} \tag{4.1}$$

respectively, where t_{imp} and t_{rel} are the impact and release times, respectively. The analytical values for these times are

$$t_{\text{imp}} = t_0 + \frac{g}{v_0}, \quad t_{\text{rel}} = t_{\text{imp}} + 2L\sqrt{\frac{\rho}{E}}, \tag{4.2}$$

where t_0 is the starting time of the simulation. Additionally, it can be shown that the contact force during impact is given by

$$f_{\text{contact}} = v_0\sqrt{E\rho}A, \tag{4.3}$$

and that the mass-averaged velocity, the kinetic energy (KE) and the potential energy (PE) take the form

$$\bar{v}(t) = \begin{cases} v_0, & t < t_{\text{imp}}, \\ v_0 - \frac{v_0\sqrt{E}}{L\sqrt{\rho}}(t - t_{\text{imp}}), & t_{\text{imp}} \le t \le t_{\text{rel}}, \\ -v_0, & t > t_{\text{rel}}, \end{cases} \tag{4.4}$$

$$KE = \begin{cases} \frac{1}{2}\rho AL v_0^2 & t < t_{\text{imp}}, \\ \frac{1}{2}\rho AL v_0^2 - \frac{1}{2}\sqrt{\rho E}A v_0^2(t - t_{\text{imp}}) & t_{\text{imp}} \le t \le t_1, \\ \frac{1}{2}\sqrt{\rho E}A v_0^2(t - t_1) & t_1 \le t \le t_{\text{rel}}, \\ \frac{1}{2}\rho AL v_0^2 & t > t_{\text{rel}}, \end{cases} \tag{4.5}$$

$$PE = \begin{cases} 0 & t < t_{\text{imp}} \\ \frac{1}{2}\sqrt{\rho E}A v_0^2(t - t_{\text{imp}}) & t_{\text{imp}} \le t \le t_1, \\ \frac{1}{2}\rho AL v_0^2 - \frac{1}{2}\sqrt{\rho E}A v_0^2(t - t_1) & t_1 \le t \le t_{\text{rel}}, \\ 0 & t > t_{\text{rel}}, \end{cases} \tag{4.6}$$

where

$$t_1 = t_{\text{imp}} + L\sqrt{\frac{\rho}{E}}, \tag{4.7}$$

is the time at which maximum PE and minimum KE are reached.

For the purpose of evaluating and comparing the various contact methods described herein, we have written a MATLAB code that discretizes the 1D impact problem using the FEM in space and the Newmark-beta time-integration scheme in time. This code is stored in an internal Sandia `git` repository. In the remainder of this document, N_x will denote the number of elements in the spatial discretization of each rod, and $\triangle t$ will denote the time-step used in the Newmark-beta time-stepper.

First, in Section 4.3, we verify the implementation of the conventional contact approaches considered herein (the penalty method and the forward increment explicit Lagrange multiplier method) on a low speed variant of the 1D impact problem, given by the parameters provided in the third column of Table 4.2. With this choice of parameters, the problem is identical to the test case considered in Section 5 of [3] and direct comparisons can be made for the purpose of verification.

Next, in Section 4.4, we evaluate the six contact methods considered herein, including our three Schwarz variants, on a high speed variant of the 1D impact problem, with parameters given in the fourth column of Table 4.2. This second high-speed variant of the 1D impact problem is qualitatively similar to the first low-speed variant, but more representative of typical Sandia applications.

TABLE 4.2
1D impact problem parameters for the two variants considered (low speed and high speed impact).

Parameter	Units	Low speed variant	High speed variant
ρ	kg/m^3	7844	1000
E	Pa	206.8×10^9	1.0×10^9
A	m^2	6.45×10^{-4}	1.0×10^{-6}
L	m	0.254	0.25
g	m	0.254×10^{-3}	0.02
v_0	m/s	5.136	100
t_s	s	0.0	-0.2×10^{-3}
t_f	s	20.0×10^{-5}	0.8×10^{-3}

4.3. Low speed impact variant: method verification. As mentioned earlier, our first task is to verify our implementation of the explicit penalty and explicit (forward increment) Lagrange multiplier (LM) methods on the low speed variant of the 1D impact problem. Toward this effect, we select parameters that match those used in the numerical study of Carpenter *et al.* [3], but converted to SI units (third column of Table 4.2). To match the setup of [3] we employed a spatial discretization having $N_x = 20$ elements, and a time-step of 2.226×10^{-6} seconds. For the explicit penalty method, we used the same value of the penalty parameter τ as the one used in [3], namely the SI equivalent of 7.5×10^6 lb/in. We did not consider the implicit penalty method, as it was not one of the methods considered in [3].

Figure 4.2 summarizes our main results for the low speed variant of the 1D impact problem (left column of the figure) compared to the results of Carpenter *et al* [3] (right column of the figure). The reader can observe that the solutions computed in our MATLAB code are qualitatively similar to those of Carpenter *et al.*, which provides verification of our implementation of these methods.

4.4. High speed impact variant: method comparison. We now evaluate the contact methods summarized in Table 4.1 on the high speed impact problem described in Section 4.2. Our main results are summarized in Figures 4.3–4.8 and Tables 4.3–4.4. In the case of the Schwarz alternating method, each rod represents its own subdomain (Ω_1 and Ω_2), as shown in Figure 4.1. Unless otherwise noted, the bars are discretized using $N_x = 200$ linear elements. Also unless otherwise noted, a time-step of $\triangle t = 1.0 \times 10^{-7}$ is employed in all methods with the exception of Implicit-Explicit Schwarz. For this Schwarz variant, we utilize a time step of $\triangle t_i$ in subdomain Ω_i with $\triangle t_1 = 1.0 \times 10^{-7}$ and $\triangle t_2 = 1.0 \times 10^{-8}$, so as to illustrate the Schwarz alternating method's ability to couple not only different time-integrators but also different time-steps in different subdomains. It was verified that the time-steps employed were small enough to ensure satisfaction of the Courant-Friedrichs-Levy (CFL) condition for the explicit methods. For all the Schwarz methods considered, a controller time-step of $\triangle T = 1.0 \times 10^{-7}$ is employed. We select very tight relative and absolute Schwarz tolerances of 1.0×10^{-15} and 1.0×10^{-12}, respectively. These tolerances are applied to the Schwarz convergence criterion, which dictates that the change of position for all the subdomains at a given Schwarz iteration be less than these relative or absolute tolerances. For the two penalty methods evaluated, we chose a penalty parameter of $\tau = 7.5 \times 10^4$, as this value yielded the most accurate results.

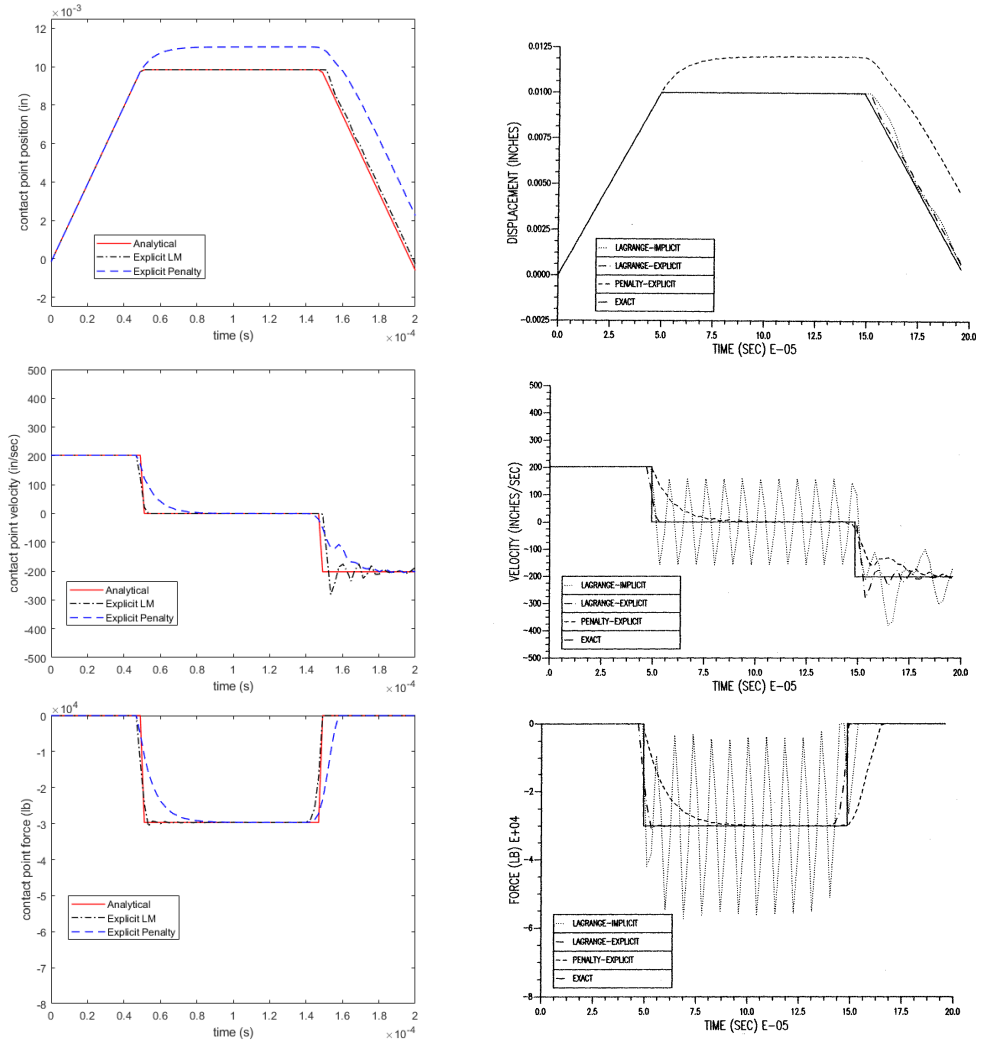

FIG. 4.2. *Contact point position, contact point velocity and contact point force solutions computed using the explicit Lagrange multiplier and explicit penalty methods in our MATLAB code (left column) compared to the published solution in [3] (right column) for the low speed impact problem.*

4.4.1. Comparison of the Schwarz alternating method to conventional contact approaches. Figure 4.3 plots the contact point location of the right-most node of the left bar (Ω_1) as a function of time. The reader can observe that both penalty methods evaluated overpredict the contact point location between the impact and release times, similar to what was seen for the low speed impact variant of this problem (Figure 4.2). This behavior is not manifested by any of the Schwarz solutions. Although small oscillations can be observed in the Schwarz solutions while the bars are in contact, these are a tiny fraction of the exact contact point location. Additionally, while all three conventional approaches underpredict the release time, the Schwarz methods capture this quantity of interest to an accuracy of $\approx 0.01\%$. Similar conclusions can be drawn from Figure 4.4, which plots the mass-averaged velocity for

the left bar as a function of time for the various methods: all three Schwarz variants calculate the mass-averaged velocity to a sufficiently greater accuracy than any of the conventional methods, especially near the time of release.

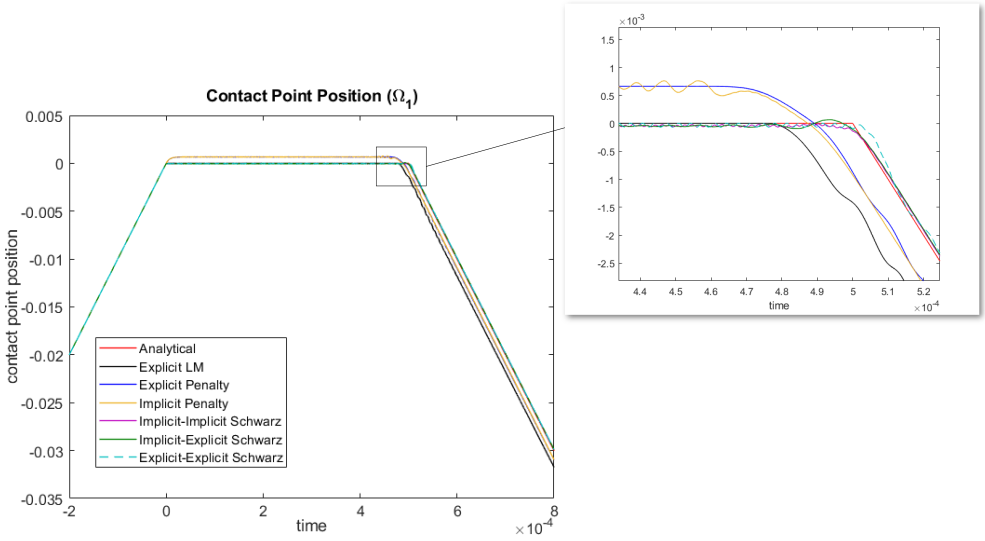

FIG. 4.3. *Contact point position for the left bar (Ω_1) as a function of time (high speed impact)*

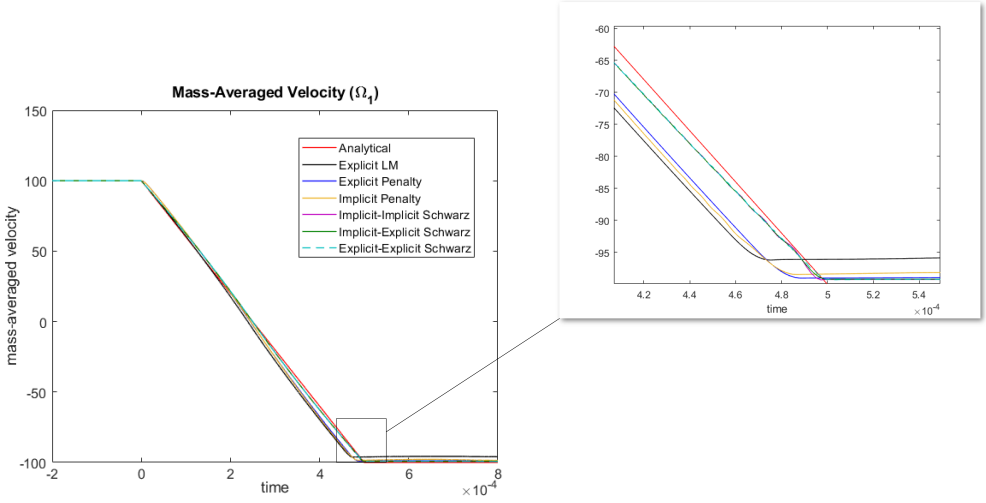

FIG. 4.4. *Mass-averaged velocity for the left bar (Ω_1) as a function of time (high speed impact)*

Figures 4.5–4.7 examine the kinetic, potential and total energies for the left bar as a function of time. It can be seen from Figure 4.5 that all three conventional methods exhibit noticeable errors in the kinetic energy after contact occurs. Halfway through the simulation, oscillations are observed in the solutions calculated using these methods. The explicit Lagrange multiplier and implicit penalty methods exhibit the largest errors in the kinetic energy following release, whereas the three Schwarz variants and the explicit penalty method exhibits the smallest error in this quantity. Remarkably,

unlike any of the conventional methods, the Schwarz method is able to track the kinetic energy with great accuracy while the bars are in contact. The Implicit-Implicit Schwarz variant delivers the most accurate and least oscillatory kinetic energy solution. Similar conclusions can be drawn by inspecting Figure 4.6, which plots the potential energy of the left bar as a function of time. What is striking about this figure is the fact that all three conventional methods underpredict the peak potential energy by approximately 10%. This behavior is not seen in the Schwarz solutions, which capture the peak potential energy with a relative error of less than 0.1%.

Next, we discuss the ability of the Schwarz alternating method to conserve the total energy, defined as the sum of the kinetic and potential energies. It is straightforward to show that the total energy should be conserved for this problem [3]. Figure 4.7 plots the total energy relative error in the left bar as a function of time for the methods evaluated. It is clear from this figure that the total energy error is negative for all six methods. This indicates that none of the methods are gaining energy, which could lead to numerical instabilities. As expected from the potential energy results (Figure 4.6), the three conventional methods exhibit a total energy loss of up to 9% following the instantiation of contact. The explicit penalty method loses the most energy, followed by the implicit penalty method and the explicit Lagrange multiplier method. Unlike the conventional contact approaches, the Schwarz method achieves an error of at most 0.25% in the total energy. It can be observed that the Explicit-Explicit Schwarz variant is the most accurate, followed by the Implicit-Implicit Schwarz and the Implicit-Explicit Schwarz. Interestingly, the more accurate Schwarz methods exhibit larger amplitude oscillations in the total energy after contact occurs.

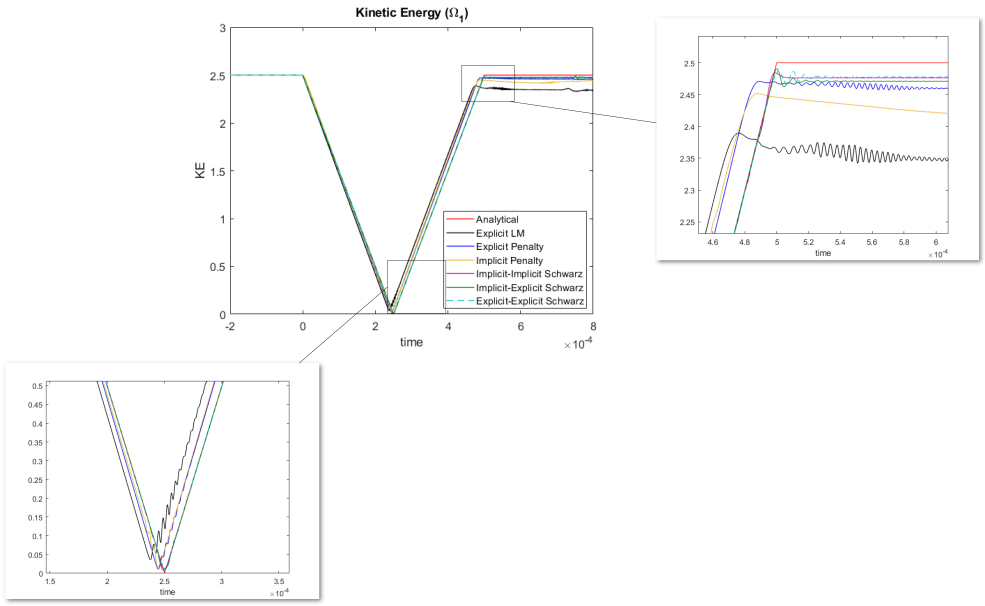

FIG. 4.5. *Kinetic energy for the left bar (Ω_1) as a function of time (high speed impact)*

In the results presented thus far, the Schwarz alternating method is better than the three conventional methods. The situation changes slightly when it comes to two other quantities of interest: the contact point force and the contact point velocity, plotted in Figures 4.8 and 4.9, respectively. While the three conventional methods ex-

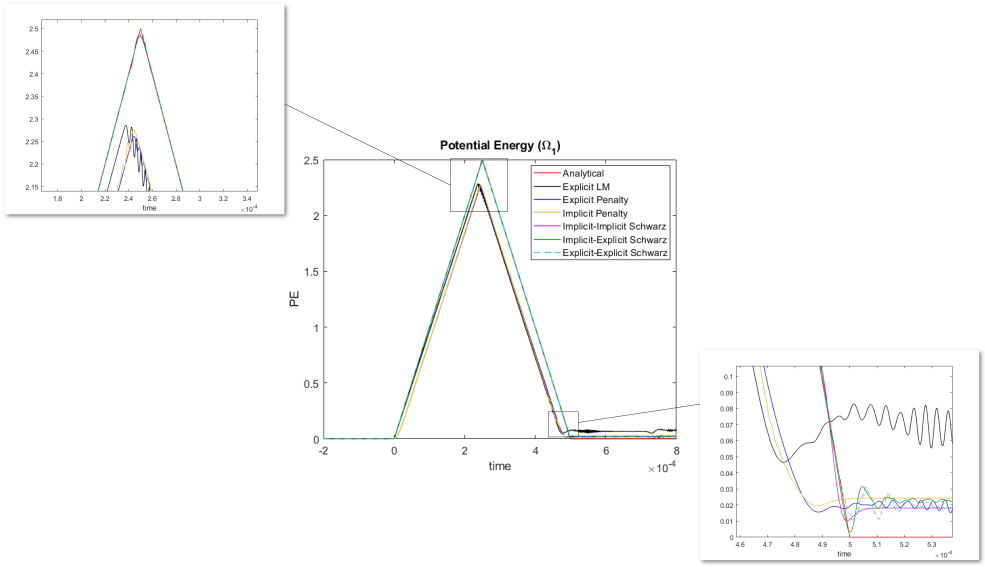

FIG. 4.6. *Potential energy for the left bar (Ω_1) as a function of time (high speed impact*

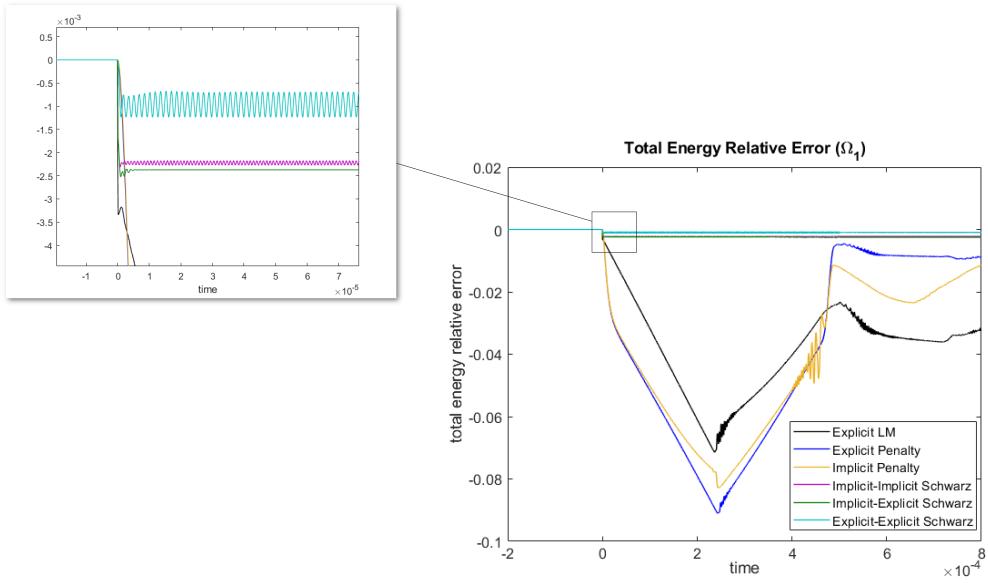

FIG. 4.7. *Relative error in the total energy for the left bar (Ω_1) as a function of time (high speed impact)*

hibit several undesirable artifacts in the contact point force (e.g., an overshoot in the contact point force at the impact time for the explicit Lagrange multiplier method, oscillations in the contact point force around the time of release for the implicit penalty method, an under-prediction of the release time; see Figure 4.8(a)), these methods deliver in general a smooth contact force solution while the bars are in contact and after the bars separate. The same cannot be said of the Schwarz solutions, which exhibit in some cases significant oscillations following the instantiation of contact

(Figure 4.8(b)). Similar results are seen in the contact point velocity (Figure 4.9), and suggest that the Schwarz methods may be suffering from a well-known problem in the simulation of mechanical contact known as chatter, in which contact is lost and reestablished, sometimes numerous times (as seen here). Numerical experiments reveal that the oscillations do not appear to be sensitive to the Schwarz convergence tolerances. It is interesting to observe that the chatter problem is significantly ameliorated by performing Implicit-Explicit Schwarz coupling. This observation suggests that the amount of chatter may be related to the predictor employed within the Schwarz coupling time integration scheme. Future work will focus on understanding the role of this predictor when it comes to the chatter problem, and potentially designing alternate predictors to reduce the amount of chatter present in the Schwarz solutions. Equally intriguing is the connection between the amount of chatter and the total energy loss (Figure 4.7). Comparing Figure 4.7 with Figures 4.8 and 4.9, it can be seen that the method with the largest total energy loss exhibits the least amount of chatter. This result is consistent with published results demonstrating that energy dissipation is necessary for the establishment of persistent contact [21], and suggests that it may be possible to reduce the amount of chatter in the Schwarz solutions by introducing numerical dissipation either through the Newmark-beta time-integrator (by selecting different parameters within this time-integration scheme) or directly into the Schwarz formulation.

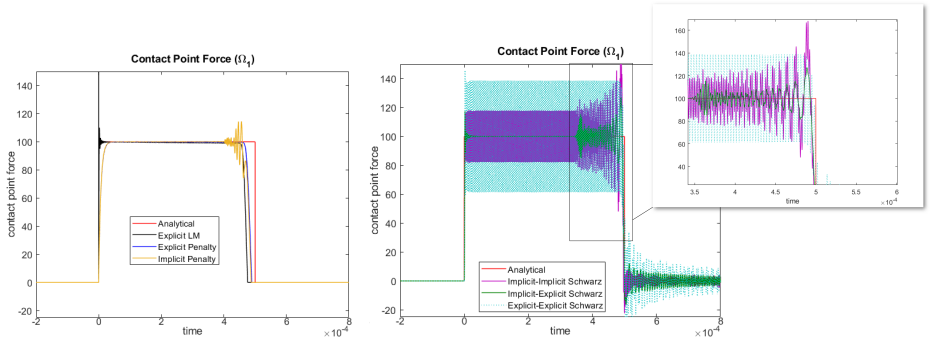

(a) Conventional methods (b) Schwarz

FIG. 4.8. *Contact point force for the left bar (Ω_1) as a function of time (high speed impact)*

4.4.2. Convergence studies of the Schwarz alternating method. Having compared the Schwarz alternating method to our three conventional methods, we now turn our attention to evaluating the former method's convergence. We consider a single quantity of interest (QOI) in this study, namely the kinetic energy in the left bar. Figures 4.10, 4.11 and 4.12 depict the convergence of the Implicit-Implicit, Implicit-Explicit and Explicit-Explicit Schwarz methods as the mesh is refined from $N_x = 50$ to $N_x = 400$ elements. For the purpose of studying convergence in space, the time-step in this study was fixed to $\triangle t = 1.0 \times 10^{-8}$ in both subdomains in these calculations. The reader can observe convergence of the computed solution to the exact analytical solution with mesh refinement for all three couplings. It is curious to remark that oscillations can be seen in the Schwarz solution calculated using the finest mesh resolution ($N_x = 400$) when performing Implicit-Explicit Schwarz coupling (Figure 4.11). These oscillations begin shortly after the onset of contact and appear to grow in time, until the bars separate. The nature of these oscillations is

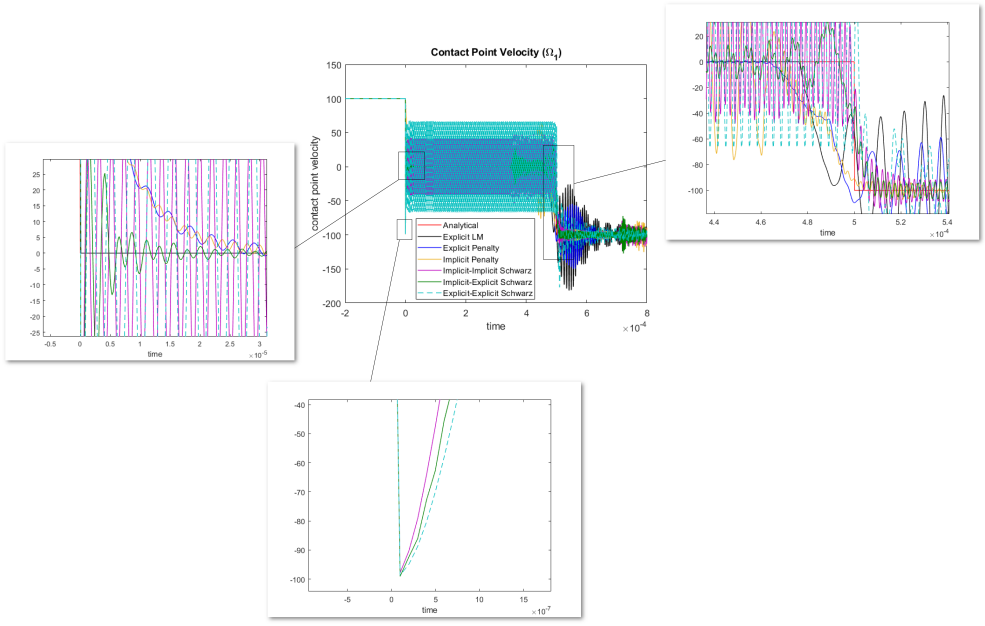

FIG. 4.9. *Contact point velocity for the left bar (Ω_1) as a function of time (high speed impact)*

currently unknown and will be studied in future work. Figure 4.13(a) depicts the mesh convergence of the three Schwarz variants considered with respect to the kinetic energy QOI. All three approaches converge at a rate of ≈ 0.82. This convergence rate is comparable to the convergence rate observed for a low-speed variant of this problem simulated using Sandia's ALEGRA code base, which implements the forward increment explicit Lagrange multiplier contact method [23]. The Explicit-Explicit Schwarz method is seen to be the most accurate, but only by a very small margin.

We lastly provide some data on the number of Schwarz iterations required for convergence, a measure of computational efficiency. Figure 4.13(b) plots the number of Schwarz iterations required for convergence for the three Schwarz variants when a spatial resolution of $N_x = 200$ and a time-step of $\triangle t = 1.0 \times 10^{-7}$ is employed. The reader can observe that the method converges in between two and five Schwarz iterations, depending on the type of coupling despite our selection of very tight Schwarz convergence tolerances (a relative tolerance of 1.0×10^{-15} and an absolute tolerance of 1.0×10^{-12}). Curiously, Explicit-Explicit Schwarz requires the fewest number of iterations to achieve convergence at this resolution (between two and three). As expected, no Schwarz iterations are required before the bars come into contact and after the bars separate. Tables 4.3 and 4.4 summarize the maximum and the average number of Schwarz iterations as a function of N_x (with a fixed time-step of $\triangle t = 1.0 \times 10^{-8}$) and as a function of $\triangle t$ (with a fixed spatial resolution of $N_x = 200$), respectively. The reader can observe that the number of Schwarz iterations increases in general as the mesh is refined. Additionally, Implicit-Implicit coupling requires the most Schwarz iterations in general. The number of Schwarz iterations required for convergence does not change significantly as the time-step is reduced, with the exception of the case in which the time-step is reduced from 1.0×10^{-7} to 1.0×10^{-8} and Explicit-Explicit Schwarz coupling is employed (Table 4.4).

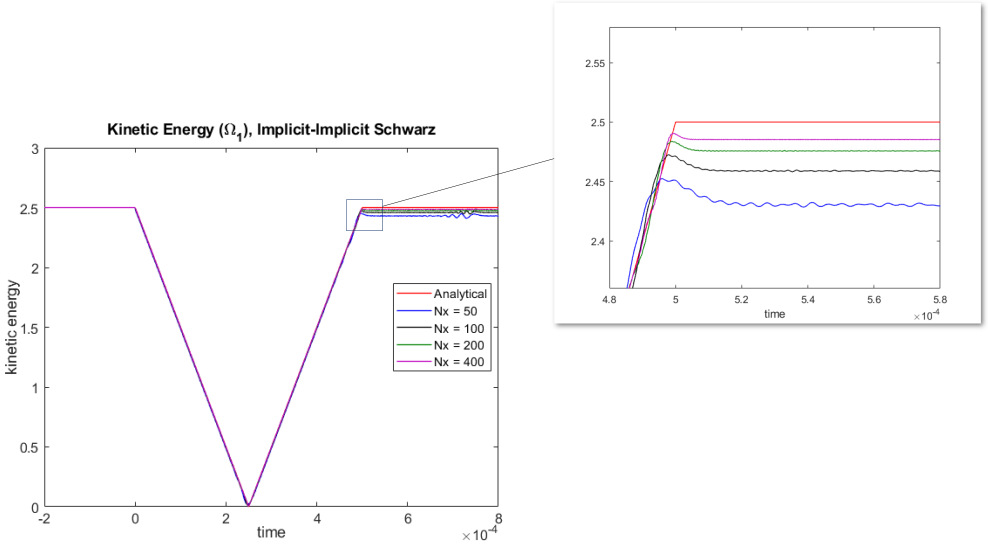

FIG. 4.10. *Mesh convergence of the kinetic energy for the left bar (Ω_1) as a function of time computing using Implicit-Implicit Schwarz coupling with a time-step of $\triangle t = 1.0 \times 10^{-8}$ in both subdomains (high speed impact).*

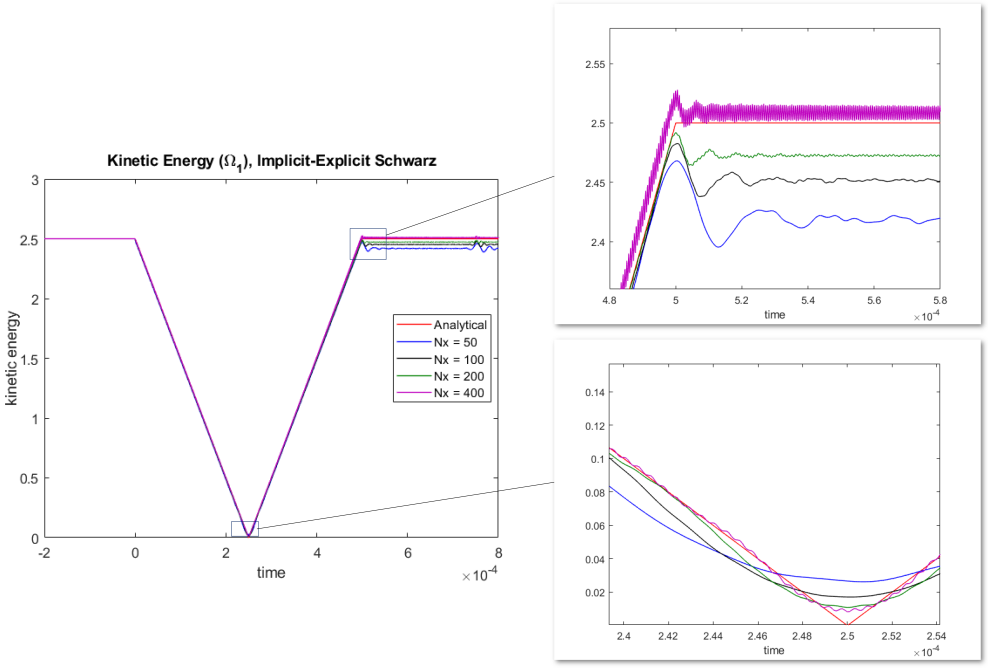

FIG. 4.11. *Mesh convergence of the kinetic energy for the left bar (Ω_1) as a function of time computing using Implicit-Explicit Schwarz coupling with a time-step of $\triangle t = 1.0 \times 10^{-8}$ in both subdomains (high speed impact).*

5. Summary. This paper presents a new computational framework for simulating mechanical contact based on the Schwarz alternating method. In this ap-

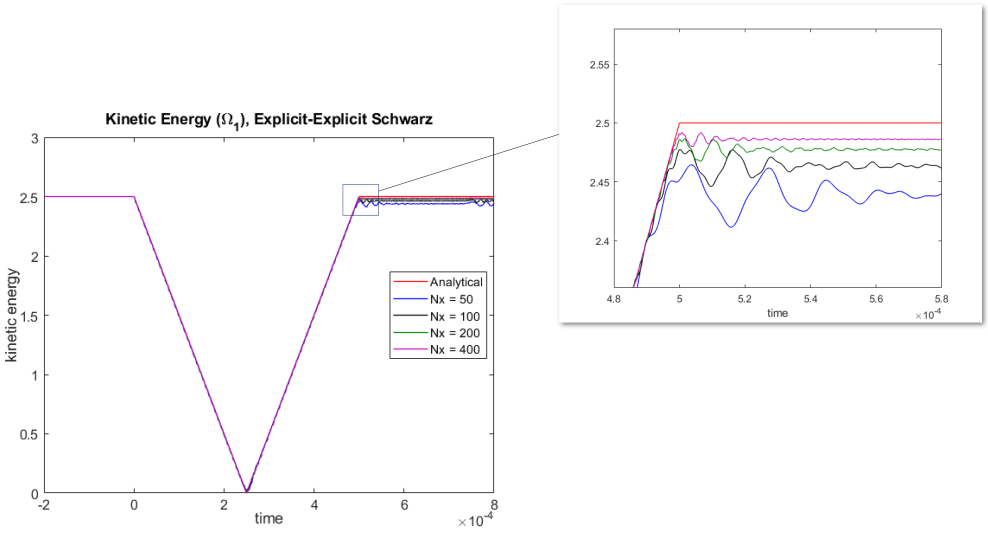

FIG. 4.12. *Mesh convergence of the kinetic energy for the left bar (Ω_1) as a function of time computing using Explicit-Explicit Schwarz coupling with a time-step of $\triangle t = 1.0 \times 10^{-8}$ in both subdomains (high speed impact).*

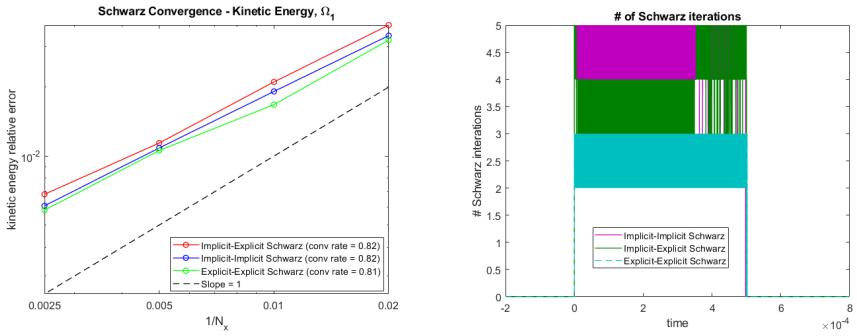

(a) Mesh convergence of the kinetic energy for the left bar (Ω_1) when $\triangle t = 1.0 \times 10^{-8}$

(b) Number of Schwarz iterations required for convergence ($N_x = 200$, $\triangle t = 1.0 \times 10^{-7}$)

FIG. 4.13. *Convergence metrics for various Schwarz couplings (high speed impact).*

TABLE 4.3
Maximum/average number of Schwarz iterations as a function of N_x with the time-step fixed to $\triangle t = 1.0 \times 10^{-8}$ for various Schwarz couplings (high speed impact).

N_x	Implicit-Implicit	Implicit-Explicit	Explicit-Explicit
50	4/1.7354	4/1.7483	4/1.7562
100	5/1.9105	4/1.7506	4/1.7569
200	5/2.2184	5/2.0225	5/2.1953
400	6/2.5882	5/2.3142	5/2.2505

proach, contact constraints are replaced with alternating Dirichlet-Neumann boundary conditions that are applied iteratively on the contact boundaries following a non-overlapping domain decomposition of the problem geometry. After describing the

TABLE 4.4
Maximum/average number of Schwarz iterations as a function of $\triangle t$ with the spatial resolution fixed to $N_x = 200$ for various Schwarz couplings (high speed impact).

$\triangle t$	Implicit-Implicit	Implicit-Explicit	Explicit-Explicit
1.0×10^{-7}	5/2.447	5/1.8768	3/1.2532
1.0×10^{-8}	5/2.2184	5/2.0225	5/2.1953
1.0×10^{-9}	5/2.2195	5/2.0607	5/2.1964

Schwarz methodology, we evaluate the method on a 1D impact problem with an exact analytical solution and compare the method's accuracy with that of conventional contact algorithms, namely the penalty method and the Lagrange multiplier method. We consider three variants of the Schwarz method in which different Newmark-beta time-integrators are used in different subdomains, so as to demonstrate the method's flexibility in coupling different time integrators with possibly disparate time-steps. Our results demonstrate the the Schwarz alternating method delivers a solution with substantially better accuracy than the conventional approaches for QOIs such as the contact point displacement, the mass-averaged velocity, the impact time, the release time, and the kinetic and potential energies. Additionally, the new method conserves energy significantly better than the conventional approaches. An unfortunate consequence of the method's ability to conserve energy so well appears to be the introduction of oscillations in the contact point velocity and contact point force. Future work will focus on better understanding the cause of these oscillations and devising approaches to mitigate them. Preliminary results suggest that the introduction of some slight dissipation [21] and/or numerical relaxation [22] can ameliorate the problem.

Future work will also include the following additional studies and extensions: (1) the introduction of additional or alternate contact constraints to those discussed in Section 3.2 to the Schwarz formulation, (2) a comparison of the Schwarz alternating method to conventional contact formulations in which a zero gap rate constraint is used in place of or in conjunction with a zero gap constraint, (3) an investigation of why the use of Implicit-Explicit Schwarz coupling introduces oscillations in QOIs such as the kinetic energy when sufficiently fine meshes are employed, and (4) an implementation and evaluation of the Schwarz alternating method in multiple spatial dimensions. The third of these tasks will require the development of operators for consistent transfer of contact traction boundary conditions using the concept of prolongation and restriction, common in multigrid methods.

Acknowledgment. Sandia National Laboratories is a multi-mission laboratory managed and operated by National Technology and Engineering Solutions of Sandia, LLC., a wholly owned subsidiary of Honeywell International, Inc., for the U.S. Department of Energy's National Nuclear Security Administration under contract DE-NA0003525. This paper describes objective technical results and analysis. Any subjective views or opinions that might be expressed in the paper do not necessarily represent the views of the U.S. Department of Energy or the U.S. Government.

REFERENCES

[1] T. BELYTSCHKO AND S. P. XIAO, *Coupling Methods for Continuum Model with Molecular Model*, International Journal for Multiscale Computational Engineering, 1 (2003), pp. 115–126.

[2] D. Boffi, F. Brezzi, and M. Fortin, *Mixed finite element methods and applications*, Springer, 2013.
[3] N. J. Carpenter, R. L. Taylor, and M. G. Katona, *Lagrange constraints for transient finite element surface contact*, International journal for numerical methods in engineering, 32 (1991), pp. 103–128.
[4] J. Côté, M. J. Gander, L. Laayouni, and S. Loisel, *Comparison of the dirichlet-neumann and optimal schwarz method on the sphere*, in Domain Decomposition Methods in Science and Engineering, T. J. Barth, M. Griebel, D. E. Keyes, R. M. Nieminen, D. Roose, T. Schlick, R. Kornhuber, R. Hoppe, J. Périaux, O. Pironneau, O. Widlund, and J. Xu, eds., Berlin, Heidelberg, 2005, Springer Berlin Heidelberg, pp. 235–242.
[5] Q. Deng, *A nonoverlapping domain decomposition method for nonconforming finite element problems*, Communications on Pure and Applied Analysis, 2 (2003), pp. 297–310.
[6] O. Faltus, *Object-oriented design and implemention of the contact mechanics into finite element code "OOFEM"*, PhD thesis, Czech Technical University, Prague, Czech Republic, 2020.
[7] D. Funaro, A. Quarteroni, and P. Zanolli, *An iterative procedure with interface relaxation for domain decomposition methods*, SIAM J. Numer. Anal., 25 (1988), pp. 1213–1236.
[8] M. Gander, *Schwarz methods over the course of time*, Electronic Transactions on Numerical Analysis, 31 (2008), pp. 228–255.
[9] L. Gerardo-Giorda and M. Perego, *Optimized schwarz methods for the bidomain system in electrocardiology*, ESAIM: Mathematical Modelling and Numerical Analysis - Modélisation Mathématique et Analyse Numérique, 47 (2013), pp. 583–608.
[10] T. Hughes, *Finite Element Method: Linear Static and Dynamic Finite Element Analysis*, Dover Publications, Inc., Mineola, New York, 2000.
[11] I. Hunek, *On a penalty formulation for contact-impact problems*, Computers and Structures, 48 (1993), pp. 193–203.
[12] F. Kwok, *Neumann–neumann waveform relaxation for the time-dependent heat equation*, in Domain Decomposition Methods in Science and Engineering XXI, J. Erhel, M. J. Gander, L. Halpern, G. Pichot, T. Sassi, and O. Widlund, eds., Cham, 2014, Springer International Publishing, pp. 189–198.
[13] P. L. Lions, *On the Schwarz alternating method III: A variant for nonoverlapping subdomains*, in Third International Symposium on Domain Decomposition Methods for Partial Differential Equations, T. F. Chan, R. Glowinski, J. Périaux, and O. B. Widlund, eds., Society for Industrial and Applied Mathematics, 1990, pp. 202–223.
[14] S. Lui, *On accelerated convergence of nonoverlapping schwarz methods*, Journal of Computational and Applied Mathematics, 130 (2001), pp. 309–321.
[15] A. Mota, I. Tezaur, and C. Alleman, *The Schwarz alternating method*, Comput. Meth. Appl. Mech. Engng., 319 (2017), pp. 19–51.
[16] A. Mota, I. Tezaur, and G. Phlipot, *The Schwarz alternating method for transient solid dynamics*, Int. J. Numer. Meth. Engng. (under review), (2021).
[17] S. S. Rao, *The finite element method in engineering*, Butterworth-heinemann, 2017.
[18] H. Schwarz, *Über einen Grenzübergang durch alternierendes verfahren*, Vierteljahrsschriftder Naturforschenden Gesellschaft in Zurich, 15 (1870), pp. 272–286.
[19] SIERRA Solid Mechanics Team, *Sierra/solidmechanics 4.22 user's guide*, Tech. Rep. SAND2011-7597, Sandia National Laboratories Report, 10 2011.
[20] J. Simo and T. Laursen, *An augmented lagrangian treatment of contact problems involving friction*, Computers and Structures, 42 (1992), pp. 97–116.
[21] J. M. Solberg and P. Papadopoulos, *A finite element method for contact/impact*, Finite Elements in Analysis and Design, 30 (1998), pp. 297–311.
[22] I. Tezaur, *Schwarz variants*, tech. rep., Unpublished manuscript, 2021.
[23] I. Tezaur, T. Voth, J. Niederhaus, J. Robbins, and J. Sanchez, *An eXtended Finite Element Method (XFEM) Formulation for Multi-Material Eulerian Solid Mechanics in the ALEGRA Code.*
[24] P. Wriggers and G. Zavarise, *Encyclopedia of Computational Mechanics, Volume 2: Solids and Structures*, John Wiley & Sons, Ltd. Edited by E. Stein, R. de Borst and T.J.R. Hughes, 2004.
[25] P. Zanolli, *Domain decomposition algorithms for spectral methods*, CALCOLO, 24 (1987), pp. 201–240.
[26] O. C. Zienkiewicz and R. L. Taylor, *The finite element method for solid and structural mechanics*, Elsevier, 2005.